

Synthesis and Characterization of Monocyclopentadienyl Titanium and Zirconium Complexes Bearing a Chelating (Chiral) Ether Side Chain on the Cp Ring

Adolphus A. H. van der Zeijden* and Chris Mattheis

*Institut für Anorganische Chemie, Martin-Luther-Universität Halle-Wittenberg,
Geusaer Strasse, D-06217 Merseburg, Germany*

Roland Fröhlich

*Organisch-Chemisches Institut der Universität Münster, Corrensstrasse 40,
D-48149 Münster, Germany*

Received January 23, 1997[®]

The compounds $(\eta^5(\eta^1)\text{-C}_5\text{H}_4\text{CH}_2\text{CH}_2\text{OR})\text{TiCl}_3$ with R = Me (**1a**), menthyl (**1b**), and fenchyl (**1c**), but not with R = isobornyl, were synthesized from the reaction of TiCl_4 and $\text{C}_5\text{H}_4(\text{CH}_2\text{CH}_2\text{OR})(\text{SiMe}_3)$ in CH_2Cl_2 . Intramolecular coordination of the ether moiety in these compounds is fluxional. From temperature-dependent NMR data in CD_2Cl_2 it was calculated that at room temperature about 30% of **1a** is in a conformation in which the ether handle is coordinated; for the chiral derivatives **1b** and **1c** this figure is significantly lower. A similar reaction using $\text{ZrCl}_4(\text{SMe}_2)_2$ yields the dimer $[(\eta^5:\eta^1\text{-C}_5\text{H}_4\text{CH}_2\text{CH}_2\text{OMe})\text{ZrCl}_2(\mu\text{-Cl})]_2$ (**2**). Chiral zirconium analogues could not be prepared in this way. The reaction of the isobornyl ligand results in selective C–O bond scission and formation of sulfonium zirconate salts. Compound **2** was structurally characterized. Probably due to its poor solubility **2** is only a moderate Ziegler–Natta catalyst for the polymerization of ethylene.

Introduction

Monocyclopentadienyl (Cp) complexes of the group 4 elements are generally more reactive than their well-investigated bis-Cp counterparts. Due to their high Lewis acidity the mono-Cp systems attract various organic substrates, which makes them ideal candidates for catalytic conversions, e.g. Diels–Alder reactions.^{1a} Of special interest to us is that these systems can be chirally modified and used for asymmetric catalysis.^{1b} However, the high reactivity of most mono-Cp complexes is accompanied by a high sensitivity to moisture,² which may lead to inactivation of catalytic properties. We are currently investigating the possibility of controlling and directing the high reactivity of the CpMCl_3 fragment by using a chelating side chain on the Cp ring bearing a (chiral) ether or amine group. Intramolecular coordination of the side chain should reduce the Lewis acidity of the metal center and enhance its stability, but at the same time it should be reactive enough to effect (asymmetric) catalytic actions.

The first mono-Cp titanium complexes bearing ether side chains were synthesized by Chinese investigators.³ These complexes were obtained by abstraction of one

of the Cp moieties from the metallocene by sulfuryl chloride. Mono-Cp titanium complexes with amine⁴ and pyridine⁵ side chains are also known, and we recently obtained the first chiral derivative.⁶ Intramolecular coordination of the side chain in most of these compounds has been secured by X-ray crystal structure determinations, all showing a square-pyramidal geometry around titanium. However, we have shown that the Ti–N coordination is dynamic in solution,⁶ and this may well be a general phenomenon for these complexes.

Several mono-Cp zirconium complexes bearing amine^{4b,c} and pyridine^{5b} side chains have been reported only very recently. We obtained the first chiral zirconium derivative and showed it to be an effective Diels–Alder catalyst.⁶ Surprisingly, there are no mono-Cp zirconium complexes known, bearing a simple ether side chain on the Cp ring. There are a few examples of tridentate, dianionic Cp/amide/ether zirconium complexes.⁷

We therefore first concentrated our investigations on the known ligand $\text{C}_5\text{H}_4\text{CH}_2\text{CH}_2\text{OMe}$ (Cp^0). We report on a simpler access to $(\eta^5\text{-Cp}^0)\text{TiCl}_3$ and on the synthesis of the analogous, novel zirconium compound. We will also describe our attempts to obtain chiral derivatives, using our recently described chiral ether ligands $\text{C}_5\text{H}_4\text{-}$

* To whom correspondence should be addressed.

® Abstract published in *Advance ACS Abstracts*, May 15, 1997.

(1) (a) Erker, G.; Sarter, C.; Albrecht, M.; Dehnicke, S.; Krüger, C.; Raabe, E.; Schlund, R.; Benn, R.; Rufinska, A.; Mynott, R. *J. Organomet. Chem.* **1990**, *382*, 89. (b) Erker, G.; van der Zeijden, A. A. H. *Angew. Chem.* **1990**, *102*, 543.

(2) (a) Hidalgo, G.; Pellighelli, M. A.; Royo, P.; Serrano, R.; Tiripicchio, A. *J. Chem. Soc., Chem. Commun.* **1990**, 1118. (b) Babcock, L. M.; Day, V. W.; Klemperer, W. G. *Inorg. Chem.* **1989**, *28*, 806.

(3) (a) Qian, Y.; Li, G.; Chen, W.; Li, B.; Jin, X. *J. Organomet. Chem.* **1989**, *373*, 185. (b) Huang, Q.; Qian, Y.; Li, G.; Tang, Y. *Transition Met. Chem.* **1990**, *15*, 483. (c) Qian, Y.; Huang, J.; Chen, X.; Li, G.; Chen, W.; Li, B.; Jin, X.; Yang, Q. *Polyhedron* **1994**, *13*, 1105.

(4) (a) Flores, J. C.; Chien, J. C. W.; Rausch, M. D. *Organometallics* **1994**, *13*, 4140. (b) Jutzi, P.; Kleimeier, J. *J. Organomet. Chem.* **1995**, *486*, 287. (c) Jutzi, P.; Siemeling, U. *J. Organomet. Chem.* **1995**, *500*, 175. (d) Herrmann, W. A.; Morawietz, M. J. A.; Priermeier, T.; Mashima, K. *J. Organomet. Chem.* **1995**, *486*, 291.

(5) (a) Clark, T. J.; Nile, T. A.; McPhail, D.; McPhail, A. T. *Polyhedron* **1989**, *8*, 1804. (b) Enders, M.; Rudolph, R.; Pritzkow, H. *Chem. Ber.* **1996**, *129*, 459.

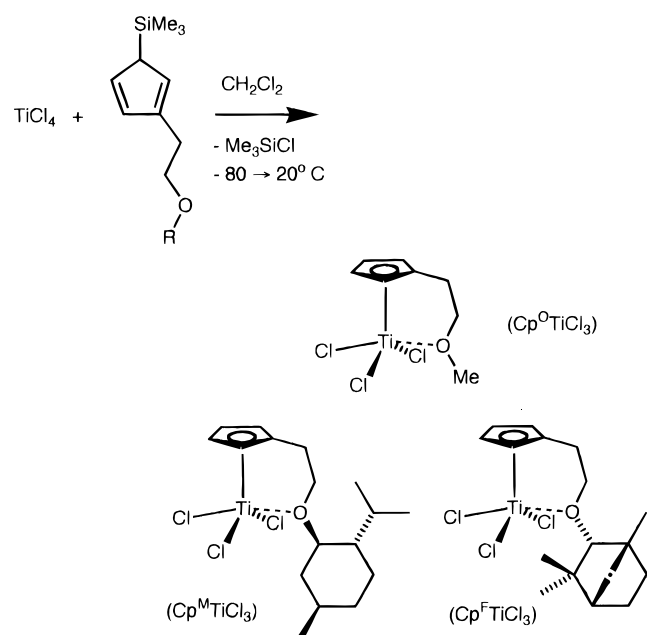
(6) van der Zeijden, A. A. H. *J. Organomet. Chem.* **1996**, *518*, 147.

(7) (a) Du Plooy, K. E.; Moll, U.; Wocadlo, S.; Massa, W.; Okuda, J. *Organometallics* **1995**, *14*, 3129. (b) Mu, Y.; Piers, W. E.; MacGillivray, L. R.; Zaworotko, M. J. *Polyhedron* **1995**, *14*, 1.

Table 1. ^1H NMR Data (ppm) of Cp^XSiMe_3 , Cp^BSnBu_3 , and $\text{Cp}^X\text{TiCl}_3^a$

compd	C_5H_4	CpCH_2	CH_2O	OCH_x	CH_3 (terpene)	SiMe ₃
Cp^OSiMe_3	3.26, 6.13, 6.42, 6.46	2.68 (t, 7.1)	3.52 (t, 7.1)	3.33 (CH_3)		-0.06
Cp^OTiCl_3	6.97	3.09 (t, 6.1)	3.75 (t, 6.1)	3.39 (CH_3)		
Cp^OTiCl_3 (-80 °C)	6.84 (2H), 7.08 (2H)	3.04 (t, 5.8)	4.29 (t, 5.8)	3.62 (CH_3)		
Cp^MSiMe_3	3.24, 6.12, 6.41, 6.47	2.68 (m,br)	3.43/3.74 ("q", 7.9)	3.03 (H_3 , m)	0.75, 0.88, 0.90	-0.06
Cp^MTiCl_3 (C_6D_6)	6.11 (2H), 6.28, 6.32	2.73 (t, 5.6)	3.09/3.51 (m)	2.78 (H_3 , m)	0.72, 0.80, 0.86	
Cp^MTiCl_3	6.97	3.09 (t, 5.8)	3.52/3.81 (dt, 9.3 × 5.8)	3.04 (H_3 , dt, 3.9 × 10.4)	0.69, 0.86, 0.92	
Cp^MTiCl_3 (-80 °C)	7.00	3.04 (s,br)	3.32/3.94 (s,br)	2.91 (H_3 , s, br)	0.48, 0.77, 0.84 (all br)	
Cp^FSiMe_3	3.26, 6.12, 6.41, 6.49	2.65 (m,br)	3.49/3.62 ("q", 7.8)	2.88 (H_2)	0.89, 1.01, 1.07	-0.06
Cp^FTiCl_3	6.98	3.09 (t, 5.8)	3.62/3.75 (dt, 9.3 × 5.8)	2.88 (H_2)	0.80, 0.98, 1.01	
Cp^FTiCl_3 (-80 °C)	7.00	3.02 (s,br)	3.47/3.62 (s,br)	2.77 (H_2)	0.61, 0.88 (2×) (all vbr)	
Cp^BSiMe_3	3.24, 6.13, 6.41, 6.48	2.64 (m,br)	3.42/3.57 ("q", 7.9)	3.21 (H_2 , m)	0.81, 0.90, 0.99	-0.07
Cp^BSnBu_3 (CDCl_3)	5.46 (2H), 6.07 (2H)	2.69 (m)	3.41/3.55 (m)	3.21 (H_2 , dd, 3.5 × 7.5)	overlap with nBu	

^a Cp^XSiMe_3 in CDCl_3 and Cp^XTiCl_3 in CD_2Cl_2 unless stated otherwise; coupling in Hz in parentheses. Only selected data for the terpene fragments are given.

Scheme 1

$\text{CH}_2\text{CH}_2\text{OR}$, with R = isobornyl (Cp^B), menthyl (Cp^M), and fenchyl (Cp^F).⁸

Results and Discussion

Titanium Compounds. The parent ($\eta^5\text{-Cp}$) TiCl_3 has been obtained in high yield by the reaction of TiCl_4 and CpSiMe_3 ,⁹ and this method has been adapted for substituted-Cp systems.^{4a,d,6} We therefore reacted $\text{Cp}^X\text{-SiMe}_3$ (X = O, B, M, F) with TiCl_4 (Scheme 1).

The compound ($\eta^5\text{-Cp}^O$) TiCl_3 (**1a**) was readily isolated using this method. The reaction for the chiral ligands had to be started at -80°C , since otherwise substantial loss of product results. Nonetheless, the isobornyl derivative Cp^BTiCl_3 could not be obtained by this method. We think there is a competing affinity of TiCl_4 for the ether linkage and the Cp moiety. At elevated temperatures this may lead to severe decomposition of the ligand because of C–O bond scission. Especially the Cp^B ligand should be prone to ether cleavage because of the relatively high stability of the resulting norbornyl carbocation (cf. reaction with ZrCl_4 ; *vide infra*).

The complexes ($\eta^5\text{-Cp}^M$) TiCl_3 (**1b**) and ($\eta^5\text{-Cp}^F$) TiCl_3 (**1c**) were obtained as yellow-brown oils, which could not be recrystallized as pure materials because of their extreme solubility. They were therefore characterized by their ^1H and ^{13}C NMR spectra (Tables 1 and 2). The Cp signals of **1b** and **1c** are very similar to those of the known **1a** and definitely identify them as mono-Cp complexes.

The solid-state structure of **1a** shows intramolecular coordination of the ether side chain.^{3b} In solution, coordination of the oxygen atom is usually expressed by low-field shifts in the NMR for the hydrogens and carbons adjacent to the oxygen atom. This is clearly seen in Table 3, in which NMR data for several Cp^O derivatives with coordinated and uncoordinated $\text{CH}_2\text{-CH}_2\text{OME}$ groups are listed. In addition, the NMR spectra of Cp^XSiMe_3 and Cp^XTiCl_3 in Tables 1 and 2 may be mutually compared. The NMR data of **1a** are strongly temperature-dependent and indicate fluxional coordination of the ether side chain (see Figure 1). Thus, at low temperature the chemical shifts for the CH_2OME moiety approach that of the coordinated side chain in [$\eta^5\text{-}\eta^1\text{-Cp}^O$] $\text{ZrCl}_2(\mu\text{-Cl})_2$, whereas at high temperature they resemble that of Cp^OH (Table 3).

The equilibrium between the two conformations is probably not attended by a high barrier. In this case the equilibrium constant K may be described by eq 1.¹⁰

From the equilibrium constants K , it is possible to

$$K = \frac{[(\eta^5\text{-Cp}^O)\text{TiCl}_3]}{[(\eta^5\text{-}\eta^1\text{-Cp}^O)\text{TiCl}_3]} = \frac{\delta - \delta_{\min}}{\delta_{\max} - \delta} \quad (1)$$

calculate thermodynamic parameters for the equilibrium according to eq 2.

$$\Delta G = -RT \ln K = \Delta H - T\Delta S \quad (2)$$

$$\ln K = \frac{\Delta S}{R} - \frac{\Delta H}{RT}$$

In order to obtain the equilibrium constants K , reasonable values for δ_{\min} and δ_{\max} are required. This was accomplished by computer-assisted iteration: δ_{\min} and δ_{\max} were optimized in such a way that plotting of $1/T$ against $\ln K$ gives the straightest line possible. By this method, the correlation coefficients were better than 0.999. For the chemical shifts of the CH_2O hydrogens

(8) van der Zeijden, A. A. H.; Mattheis, C. *Synthesis* **1996**, 847.

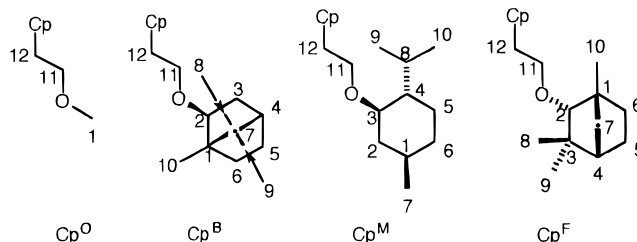
(9) Cardoso, A. M.; Clark, R. J. H.; Moorhouse, S. *J. Chem. Soc., Dalton Trans.* **1980**, 1156.

(10) Dalling, D. K.; Zilm, K. W.; Grant, D. M.; Heeschen, W. A.; Horton, W. J.; Pugmire, R. J. *J. Am. Chem. Soc.* **1981**, 103, 4817.

Table 2. ^{13}C NMR Data (ppm) of $\text{Cp}^{\text{X}}\text{SiMe}_3$, $\text{Cp}^{\text{B}}\text{SnBu}_3$, and $\text{Cp}^{\text{X}}\text{TiCl}_3^{\text{a}}$

compd	C ₁	C ₂	C ₃	C ₄	C ₅	C ₆	C ₇	C ₈	C ₉	C ₁₀	CH ₂ O	CH ₂ Cp	C (Cp)	SiMe ₃
$\text{Cp}^{\text{O}}\text{SiMe}_3$	58.34										72.78	30.12	51.24, 128.4, 132.0, 133.8, 141.7	-2.19
$\text{Cp}^{\text{O}}\text{TiCl}_3$	59.64										73.24	31.86	122.86 (2C), 124.74 (2C), 143.57	
$\text{Cp}^{\text{O}}\text{TiCl}_3^{\text{b}}$	62.45										79.11	29.46	124.39 (2C), 124.72 (2C), 145.88	
$\text{Cp}^{\text{M}}\text{SiMe}_3$	31.56	40.58	79.14	48.29	23.44	34.62	22.34	25.55	16.28	20.95	68.59	30.91	51.13, 128.2, 132.2, 133.6, 142.0	-2.11
$\text{Cp}^{\text{M}}\text{TiCl}_3$	31.83	40.74	79.90	48.61	23.63	34.90	22.53	25.97	16.42	21.11	67.48	33.34	124.53, 124.62, 124.68, 125.10, 143.52	
$\text{Cp}^{\text{M}}\text{TiCl}_3^{\text{c}}$	30.8	39.2	79.0	47.4	22.0	33.8	22.0	24.7	15.2	20.6	67.1	32.3	124.2, 124.6, 124.8, 125.2, 143.4	
$\text{Cp}^{\text{F}}\text{SiMe}_3$	49.10	93.13	39.45	48.72	26.19*	25.97*	41.42	31.74	20.72	20.07	72.11	30.81	51.17, 128.3, 132.5, 133.6, 141.8	-2.05
$\text{Cp}^{\text{F}}\text{TiCl}_3$	49.52	93.87	39.85	49.15	26.44*	26.34*	41.62	31.80	20.87	20.24	71.09	33.44	124.63 (2C), 125.14 (2C), 143.54	
$\text{Cp}^{\text{F}}\text{TiCl}_3^{\text{c}}$	48.5	91.9	38.7	47.9	25.6*	25.2*	40.4	31.1	20.0	19.6	70.1	32.5	124.68 (2C), 125.16 (2C), 143.33	
$\text{Cp}^{\text{B}}\text{SiMe}_3$	49.21	87.23	38.73	45.19	27.41	34.60	46.43	20.26*	20.31*	11.94	69.66	30.88	51.16, 128.20, 132.62, 133.47, 142.61	-2.04
$\text{Cp}^{\text{B}}\text{SnBu}_3$	49.20	87.21	38.79	45.19	27.40	34.61	46.45	20.31 (2C)		11.95	70.26	30.93	97.95, 98.15, 118.49, 118.76, 139.00	

^a $\text{Cp}^{\text{X}}\text{SiMe}_3$ in CDCl_3 , $\text{Cp}^{\text{X}}\text{TiCl}_3$ in CD_2Cl_2 ; measured at room temperature, unless stated otherwise. Cp signals of SiMe_3 derivatives are broad. Signals marked with asterisks may have been interchanged. Numbering system:



^b At -40 °C. ^c At -80 °C; all signals broad.

Table 3. ^1H and ^{13}C NMR Data (ppm) of $\text{C}_5\text{H}_4\text{CH}_2\text{CH}_2\text{OME}$ (Cp^{O}) Derivatives

compd	solvent	CpCH_2^{a}	$\text{CH}_2\text{O}^{\text{a}}$	OCH_3	CpCH_2	CH_2O	OCH_3	lit.
O-Coordinated								
$[\text{Cp}^{\text{O}}\text{ZrCl}_2(\mu\text{-Cl})_2]$	CDCl_3	2.92 (6.3)	4.33 (6.3)	3.75	27.5	82.3	64.8	this work
$[\text{Cp}^{\text{O}}_2\text{La}(\mu\text{-Cl})_2]$	$\text{THF-}d_8$	2.60	3.60	3.40	32.5	79.3	62.4	<i>b</i>
$\text{Cp}^{\text{O}}_2\text{YCl}$	$\text{THF-}d_8$	2.54	3.80	3.42	30.8	80.4	64.5	<i>b</i>
	$\text{THF-}d_8$	2.65	3.91	3.52	29.74	79.40	not given	<i>c</i>
$\text{Cp}^{\text{O}}_2\text{Y}(\text{AlH}_4)$	C_6D_6	2.27	3.27	3.09	29.45	78.16	60.81	<i>c</i> (^{13}C NMR in $\text{THF-}d_8$)
$\text{Cp}^{\text{O}}_2\text{Y}(\text{BH}_4)$	C_6D_6	2.32	3.29	3.11	28.99	78.67	62.87	<i>c</i> (^{13}C NMR in C_7D_8)
$[\text{Cp}^{\text{O}}_2\text{Y}(\mu\text{-H})_2]$	C_6D_6	2.56	3.35	3.06	30.29	77.66	60.73	<i>c</i>
Not O-Coordinated								
$\text{Cp}^{\text{O}}\text{H}^{\text{i}}$	CDCl_3	2.61	3.49	3.29	30.4	72.1	58.2	this work
$\text{Cp}^{\text{O}}_2\text{TiCl}_2$	CDCl_3	2.96 (6.1)	3.59 (6.1)	3.31	31.1	72.0	58.6	<i>d</i>
$\text{Cp}^{\text{O}}_2\text{ZrCl}_2$	CDCl_3	2.91 (6.2)	3.58 (6.2)	3.34	30.3	72.2	58.4	<i>h</i>
$\text{Cp}^{\text{O}}_2\text{Fe}$	CDCl_3	2.54 (7.1)	3.43 (7.1)	3.30	29.4	73.3	58.2	<i>e</i>
$\text{Cp}^{\text{O}}\text{Ir}(\text{CO})_2$	CDCl_3	2.61	3.51	3.35	27.7	75.1	58.6	<i>f</i>
$\text{Cp}^{\text{O}}\text{Mn}(\text{CO})_3$	CDCl_3	2.48	3.47	3.33	28.4	72.7	58.6	<i>g</i>

^a Triplet; $^3J_{\text{HH}}$ in parentheses, when given in the original literature. ^b Qian, C.; Wang, B.; Deng, D.; Hu, J.; Chen, J.; Wu, G.; Zheng, P. *Inorg. Chem.* **1994**, *33*, 3382. ^c Laske, D. A.; Duchateau, R.; Teuben, J. H. *J. Organomet. Chem.* **1993**, *462*, 149. ^d Reference 3b. ^e Rees, W. S.; Lay, U. W.; Dippel, K. A. *J. Organomet. Chem.* **1994**, *483*, 27. ^f Blais, M. S.; Rausch, M. D. *J. Organomet. Chem.* **1995**, *502*, 1. ^g Yeh, P.-H.; Pang, Z.; Johnston, R. F. *J. Organomet. Chem.* **1996**, *509*, 123. ^h Reference 22. ⁱ Signals of the two isomers were averaged.

in CD_2Cl_2 , the best fits are obtained using values for δ_{max} of 4.35 and δ_{min} of 3.51 ppm. These values correspond very well with those in $[(\eta^5\text{-}\eta^1\text{-Cp}^{\text{O}})\text{ZrCl}_2(\mu\text{-Cl})_2]$ (4.33 ppm in CDCl_3) and in $\text{Cp}^{\text{O}}\text{H}$ (3.49 ppm). From these data one obtains $\Delta H = +16.8(2)$ kJ/mol and $\Delta S = +65.4(10)$ J/(mol/K). A similar procedure was followed for the chemical shifts of the OCH_3 hydrogens. With δ_{max} 3.64 and δ_{min} 3.27 ppm one finds $\Delta H = +17.6(5)$ kJ/mol and $\Delta S = +67.2(15)$ J/(mol/K) (correlation coefficient 1.000). These data are in excellent agreement with each other. The ^{13}C data for CH_2OCH_3 give similar results. The best fits are obtained with δ_{max} 83.6

and δ_{min} 69.6 ppm for CH_2O and δ_{max} 64.7 and δ_{min} 57.7 ppm for OCH_3 .

The large positive value of ΔS is in agreement with decomplexation of the ether handle in the forward reaction in Figure 1, and the low value of ΔH indicates a weak Ti–O bond. It is noticed that the parent $(\eta^5\text{-Cp})\text{TiCl}_3$ does not form a complex with thf.⁹ At ca. -13 °C the equilibrium constant K equals 1, and there are just as many conformers with a coordinated ether handle as there are without. At room temperature ($+21$ °C) about 30% of **1a** is in a conformation in which the ether handle is coordinated.

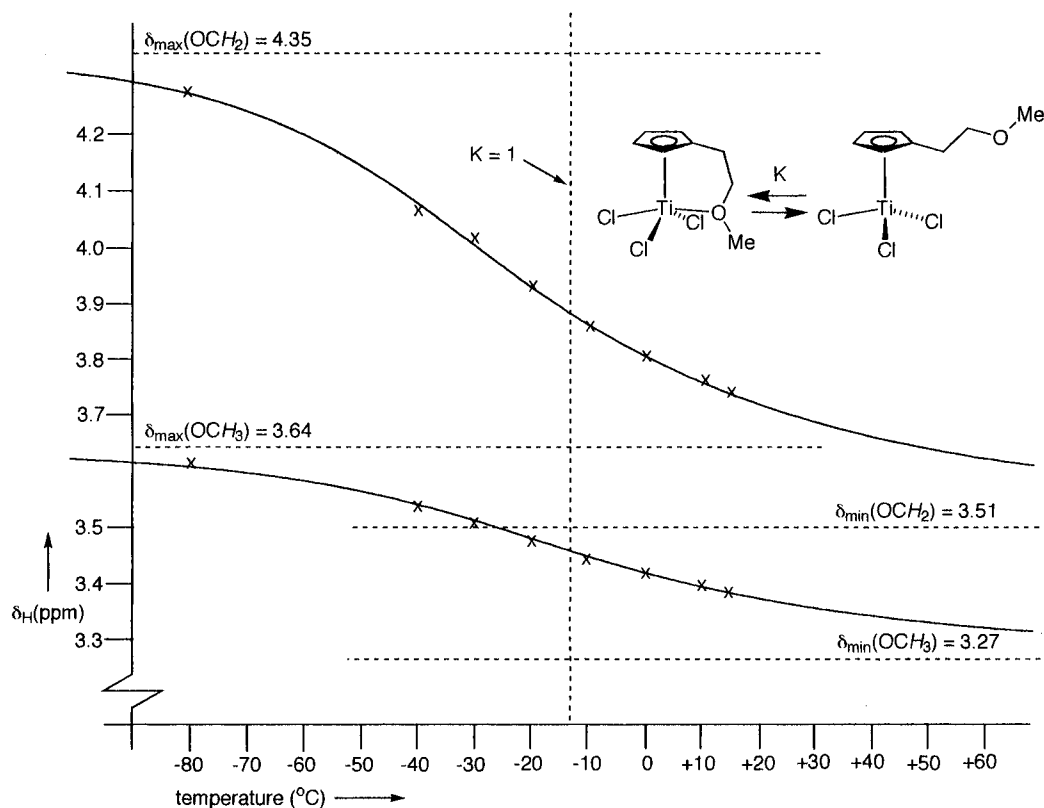


Figure 1. Temperature dependent ^1H NMR of $[\eta^5(\text{:}\eta^1\text{-Cp}^0)]\text{TiCl}_3$ (**1a**) in CD_2Cl_2 . The measured chemical shifts for the CH_2OCH_3 hydrogens are denoted with (x).

For the chiral derivatives **1b** and **1c** the NMR data of the CH_2OCHR_2 moiety are close to those of their SiMe_3 precursor. Therefore, the equilibrium lies even more to the side of the uncoordinated conformation. Even at -80°C the NMR data are not very different from those at room temperature (Tables 1 and 2). It is probably the larger steric bulk of the terpene moieties in these compounds that prevents facile ether coordination.

Clearly, the intramolecular coordination of the ether side chain is not very strong in **1**. Therefore, it is to be expected that during a Diels–Alder reaction the ether moiety will be displaced by substrate molecules during catalysis. Significant chiral induction through the ligand system thereby seems unlikely, and we therefore concentrated our further efforts on the analogous zirconium systems.

Zirconium Compounds. The synthetic procedure used for the preparation of mono-Cp titanium compounds is not so easily adapted for zirconium. Whereas the reaction of ZrCl_4 or $\text{ZrCl}_4(\text{OR})_2$ with CpSiMe_3 does not afford mono-Cp zirconium compounds, it was recently discovered that the use of ZrCl_4 sulfide complexes gives excellent results.¹¹ Accordingly, from the reaction of $\text{ZrCl}_4(\text{SMe}_2)_2$ with Cp^0SiMe_3 in CH_2Cl_2 $[\eta^5\text{:}\eta^1\text{-Cp}^0)\text{-ZrCl}_2(\mu\text{-Cl})_2$ (**2**) crystallizes out within a few hours in about 80% yield (Scheme 2).

The colorless compound is hygroscopic and should be stored under an inert atmosphere. Single crystals of **2**

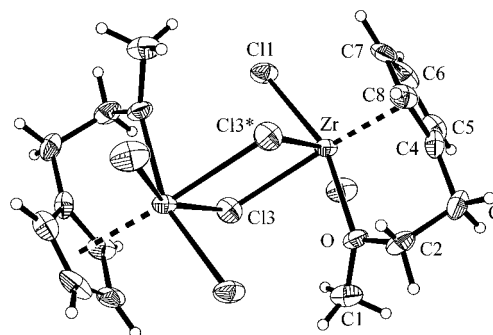
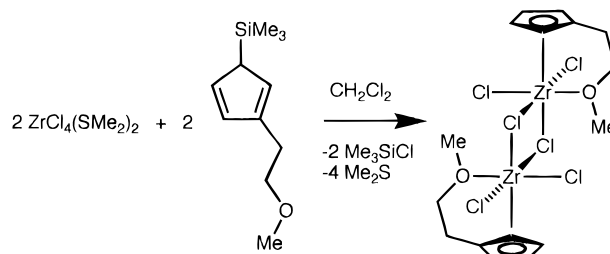


Figure 2. Molecular structure of **2**.

Scheme 2



were analyzed by X-ray diffraction. Crystal data are listed in Table 4. Selected bond lengths and angles are given in Table 5. The structural analysis shows that **2** is composed of chloride-bridged dimers in the solid state (Figure 2).

The dimer possesses a crystallographically imposed inversion center and the molecule consists of two edge-sharing distorted octahedrons. This arrangement is very similar to that in other six-coordinate, chloride-bridged compounds such as $[\eta^5\text{-CpZrCl}_2(\text{EtC}(\text{O})\text{Me})(\mu\text{-Cl})_2]$ (**3a**),¹² $[\eta^5\text{-CpZrCl}_2(\text{EtOC}(\text{O})\text{Me})(\mu\text{-Cl})_2]$ (**3b**),¹² and

(11) (a) Lund, E. C.; Livinghouse, T. *Organometallics* **1990**, *9*, 2426. See also: (b) Fryzuk, M. D.; Mao, S. S. H.; Zaworotko, M. J.; MacGillivray, L. R. *J. Am. Chem. Soc.* **1993**, *115*, 5336. (c) Fryzuk, M. D.; Mao, S. S. H.; Duval, P. B.; Rettig, S. J. *Polyhedron* **1995**, *14*, 11. (d) Willey, G. R.; Butcher, M. L.; Drew, M. G. B. *J. Chem. Soc., Dalton Trans.* **1994**, 3285.

Table 4. Crystallographic Data for $[(\eta^5\text{-}\eta^1\text{-C}_5\text{H}_4\text{CH}_2\text{CH}_2\text{OMe})\text{ZrCl}_2(\mu\text{-Cl})_2$ (2**)**

chem formula	C ₈ H ₁₁ Cl ₃ OZr
cryst dimens, mm	0.25 × 0.25 × 0.20
mol wt	320.74
cryst syst	monoclinic
space group	<i>P</i> 2 ₁ / <i>c</i>
<i>a</i> , Å	10.572(1)
<i>b</i> , Å	7.989(1)
<i>c</i> , Å	14.002(1)
α, deg	90
β, deg	111.92(1)
γ, deg	90
<i>V</i> , Å ³	1097.1(2)
<i>Z</i>	4
<i>d</i> _{calc} , g cm ⁻³	1.942
μ(Mo Kα), cm ⁻¹	16.9
<i>F</i> (000)	632
<i>T</i> , K	173
θ range, deg	2.99–26.29
no. of rflns measd	2315
no. of indep rflns	2220
no. of obsd rflns (<i>I</i> > 2σ(<i>I</i>))	1448
<i>R</i> (<i>I</i> > 2σ(<i>I</i>))	0.049
w <i>R</i> 2 (<i>I</i> > 2σ(<i>I</i>))	0.114

Table 5. Selected Bond Distances (Å) and Angles (deg) for $[(\eta^5\text{-}\eta^1\text{-C}_5\text{H}_4\text{CH}_2\text{CH}_2\text{OMe})\text{ZrCl}_2(\mu\text{-Cl})_2$ (2**)**

Zr–Cl(1)	2.455(2)	Zr–C(6)	2.498(7)
Zr–Cl(2)	2.472(2)	Zr–C(7)	2.508(6)
Zr–Cl(3)	2.642(2)	Zr–C(8)	2.517(6)
Zr–Cl(3)*	2.562(2)	O–C(1)	1.450(9)
Zr–O	2.264(4)	O–C(2)	1.446(8)
Zr–C(4)	2.522(6)	C(2)–C(3)	1.501(10)
Zr–C(5)	2.512(7)	C(3)–C(4)	1.493(9)
Cl(1)–Zr–Cl(2)	91.71(7)	Cl(3)–Zr–O	78.46(12)
Cl(1)–Zr–Cl(3)	81.51(6)	Cl(3)*–Zr–O	83.52(13)
Cl(1)–Zr–Cl(3)*	90.81(7)	Zr–Cl(3)–Zr*	103.17(7)
Cl(1)–Zr–O	159.93(13)	Zr–O–C(1)	127.6(4)
Cl(2)–Zr–Cl(3)	78.10(7)	Zr–O–C(2)	117.8(4)
Cl(2)–Zr–Cl(3)*	154.13(7)	C(1)–O–C(2)	113.5(5)
Cl(2)–Zr–O	85.36(13)	O–C(2)–C(3)	107.6(5)
Cl(3)–Zr–Cl(3)*	76.83(7)	C(2)–C(3)–C(4)	109.0(5)

$[(\eta^5\text{-}\eta^1\text{-C}_5\text{Me}_4\text{C}_9\text{H}_6\text{N})\text{ZrCl}_2(\mu\text{-Cl})_2$ (**4**).^{5b} In all of these complexes the chloride atoms *trans* to Cp and Cl are involved in bridging. The geometry is also similar to that in the six-coordinate hydroxy-bridged dimers $[\eta^5\text{-CpZr}(\text{H}_2\text{O})_3(\mu\text{-OH})_2]^{4+}$ (**5**)¹³ and $[(\eta^5\text{-Cp}^*)\text{ZrCl}_2(\text{H}_2\text{O})(\mu\text{-OH})_2]$ (**6**)¹⁴ or in the five-coordinate chloride-bridged dimers $[(\eta^5\text{-Cp}^*)\text{ZrCl}_2(\mu\text{-Cl})_2]^{15}$ and $[(\eta^5\text{-C}_9\text{H}_7)\text{HfCl}_2(\mu\text{-Cl})_2]^{16}$. The terminal Zr–Cl distances (2.455(2) and 2.472(2) Å) resemble those in **3a** (2.461(1) and 2.463(1) Å), **3b** (2.456(1) and 2.476(1) Å), and **4** (2.444(5) and 2.466(5) Å). The bridging Zr–Cl distances are significantly longer than the terminal ones. The bridge is asymmetric, because the *trans*-Cp distance (2.642(2) Å) is longer than the *trans*-Cl distance (2.562(2) Å). A similar situation is encountered in **3a** (2.727(1) vs 2.579(1) Å), **3b** (2.726(1) vs 2.576(1) Å), and **4** (2.684(6) vs 2.524(6) Å). The hydroxy-bridged derivatives **5** (Zr–O_{*trans*}-Cp = 2.160(2) Å vs Zr–O_{*trans*}-O = 2.075(3) Å) and **6** (2.232(3) vs 2.081(3) Å) show similar asymmetric distortions, which can be ascribed to a higher *trans* effect of the Cp ligand in comparison with that of Cl and O atoms.

(12) Erker, G. *J. Organomet. Chem.* **1990**, *400*, 185.(13) Lasser, W.; Thewalt, U. *J. Organomet. Chem.* **1986**, *311*, 69.(14) Hidalgo, G.; Pellighelli, M. A.; Royo, P.; Serrano, R.; Tiripicchio, A. *J. Chem. Soc., Chem. Commun.* **1990**, 1118.(15) Martin, A.; Mena, M.; Palacios, F. *J. Organomet. Chem.* **1994**, *480*, C10.(16) Shaw, S. L.; Morris, R. J.; Huffman, J. C. *J. Organomet. Chem.* **1995**, *489*, C4.

The three bond angles around the oxygen atom add up to 358.9°, indicating sp² hybridization; the oxygen atom acts as a four-electron σ,π-donor, which is very common for electron-deficient elements. The chelating CH₂CH₂OMe moiety is puckered. The methyl carbon C(1) seems to be pushed away by Cl(1)* of the opposing zirconium unit, which is 3.615(2) Å away. This is expressed by the torsion angle Cl(2)–Zr–O–C(1) of only –31.2(6)°. Consequently, the methylene carbon C(2) points in the other direction (torsion angle Cl(2)–Zr–O–C(2) = 136.5(4)°).

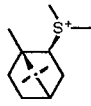
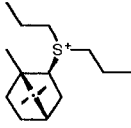
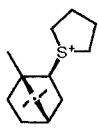
The parent unsubstituted Cp derivative $[\eta^5\text{-CpZrCl}(\mu\text{-Cl})_2]_n$ is an insoluble polymer.¹⁷ The presence of the oxygen side arm in **2** prevents the structure from being polymeric. Therefore, **2** is soluble in various solvents. It is moderately soluble in CHCl₃ and MeCN, slightly soluble in CH₂Cl₂, benzene, toluene, thf, and acetone, and insoluble in alkanes and diethyl ether. It is very soluble in DMSO, methanol, and even water.¹⁸

The C_i dimeric structure of **2** is not maintained in solution. For that structure, the arrangement requires four different resonances for the two CH₂ groups in the ¹H NMR, as well as four resonances of the Cp ring hydrogens. Instead, two triplet signals are observed for both CH₂ groups as well as two signals for the Cp H atoms down to –50 °C in CD₂Cl₂ (below this temperature no more signals for **2** were observed, probably because of precipitation). The ¹H and ¹³C NMR spectra show strong downfield shifts for the CH₂OMe signals with respect to those of the free ligand, indicating that the ether handle remains coordinated to the zirconium center in solution (Table 3). These data are only consistent with a *monomeric* molecule with C_s symmetry, and therefore, the barrier to dimer–monomer dissociation must be quite low.

After the successful preparation of **2**, we also attempted to synthesize the promising chiral analogues by using the ligands Cp^BH, Cp^MH, and Cp^FH mentioned earlier. Unfortunately, by the same procedure as for Cp^OZrCl₃, the reaction of ZrCl₄(SMe₂)₂ with either Cp^M-SiMe₃ or Cp^F-SiMe₃ does not lead to isolable compounds, whereas ZrCl₄(thf)₂ does not react with Cp^X-SiMe₃. However, the similar reaction of ZrCl₄(SR₂)₂ (R = Me, Pr, C₄H₈ (tetrahydrothiophene, THT)) with Cp^B-SiMe₃ or Cp^B-SnBu₃ in CH₂Cl₂ or toluene proceeds more cleanly. A grayish white material was isolated. The ¹H and ¹³C NMR data show one set of signals for the isobornyl group and one set of SR₂ signals (integrating 1:1 with the isobornyl group) but at least two sets of signals for the Cp unit present in various ratios (Tables 6 and 7). Surprisingly, in the isobornyl group the chemical shift of C₂ (62–65 ppm) as well as its ¹J_{CH} coupling of ca. 155 Hz is not consistent with an oxygen atom attached to it but, rather, to a sulfur atom. The NMR signals of the sulfide groups are also unexpected. For instance, the Me₂S species has diastereotopic signals for the methyl hydrogens and carbons, suggesting the proximity of a *chiral* group. We therefore think that the sulfide and isobornyl units in the product are linked in a *sulfonium* cation, R₂(isobornyl)S⁺ (S⁺). Such a cation can be synthesized much more simply by starting

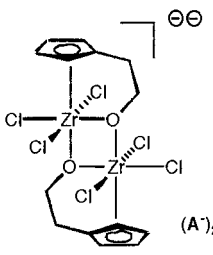
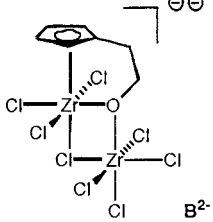
(17) Engelhardt, L. M.; Papasergio, R. I.; Raston, C. L.; White, A. H. *Organometallics* **1984**, *3*, 18.(18) The coordination chemistry of **2** will be the subject of a forthcoming paper: van der Zeijden, A. A. H.; Mattheis, C.; Fröhlich, R.; Dippel, F. Submitted for publication.

Table 6. NMR Data of Isobornyl Sulfonium Cations^a

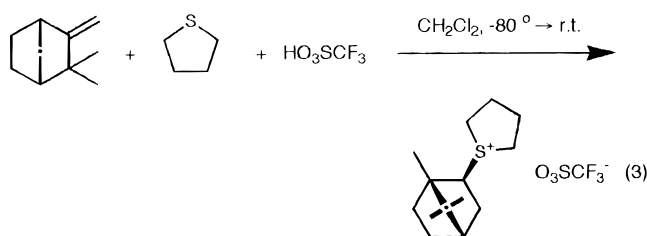
Compound	δ (ppm)
	¹ H NMR: 0.89/0.97/1.11 (3x3H, H _{8/9/10}), 3.69 (1H, m, H ₂), 0.8-2.2 (m, 7H), 2.98/3.10(2x3H, S(CH ₃)). ¹³ C NMR: 50.95 (C ₁), 64.98 (C ₂ , d, 153), 37.29 (C ₃ , t, 133), 45.03 (C ₄ , d, 144), 26.46 (C ₅ , t, 135), 34.32 (C ₆ , t, 132), 48.64 (C ₇), 19.79 (C _{8/9} , q, 126), 14.37 (C ₁₀ , q, 126), 25.56/29.42 (S(CH ₃) ₂ , q, 149)
	¹ H NMR: 0.89/0.94/1.10 (3x3H, H _{8/9/10}), 4.01 (1H, m, H ₂), 0.8-2.2 (m, 17H), 3.28 (m, 2H)/3.50 (m, 1H)/3.82 (m, 1H), (all S(CH ₂ CH ₂ CH ₃) ₂). ¹³ C NMR: 50.88 (C ₁), 62.27 (C ₂ , d, 156), 37.16 (C ₃ , t, 135), 45.07 (C ₄ , d, 137), 26.32 (C ₅ , t, 131), 34.20 (C ₆ , t, 135), 48.79 (C ₇), 19.66/19.78 (C _{8/9} , d, 127), 14.17 (C ₁₀ , q, 126), 13.08 (SCH ₂ CH ₂ CH ₃ , q, 129), 19.57/19.72 (SCH ₂ CH ₂ , t, 127), 41.67/45.97 (SCH ₂ , t, 145)
	¹ H NMR: 0.90/1.03/1.11 (3x3H, H _{8/9/10}), 3.55 (1H, m, H ₂), 0.8-2.5 (m, 11H), 3.72/3.45 (2x2H, m, S(CH ₂ R) ₂). ¹³ C NMR: 50.45 (C ₁), 63.10 (C ₂ , d, 154), 37.12 (C ₃ , t, 143), 45.12 (C ₄ , d, 141), 26.47 (C ₅ , t, 133), 35.17 (C ₆ , t, 136), 48.69 (C ₇), 19.89/19.94 (C _{8/9} , q, 124), 14.35 (C ₁₀ , q, 125), 28.58/29.48 (SCH ₂ CH ₂ , t, 133), 42.94, 46.45 (SCH ₂ , t, 150)

^a In CDCl₃. For numbering system, see Table 1. ¹J_{CH} (in Hz) in parentheses.

Table 7. NMR Data of Zirconate Anions in CDCl₃

Compound	δ (ppm)
	¹ H NMR: 2.85 (2H, br, CpCH ₂), 4.85 (2H, br, CH ₂ O), 6.32/6.49 (2x2H, C ₅ H ₄) ¹³ C NMR: 30.23 (CpCH ₂ , t, 127), 82.24 (CH ₂ O, t, 147), 115.24 (C ₅ H ₄ , d, 174), 120.15 (C ₅ H ₄ , d, 175), 135.49 (C ₅ H ₄)
	¹ H NMR: 2.97 (2H, t, 6.0, CpCH ₂), 5.09 (2H, t, 6.0, CH ₂ O), 6.49/6.70 (2x2H, C ₅ H ₄) ¹³ C NMR: 29.07 (CpCH ₂ , t, 129), 85.73 (CH ₂ O, t, 149), 116.83 (C ₅ H ₄ , d, 174), 122.28 (C ₅ H ₄ , d, 175), 137.65 (C ₅ H ₄)

with camphene (eq 3). The sulfonium salt [THT-



(isobornyl)][O₃SCF₃] obtained in this way has NMR characteristics identical with those of the species obtained by the zirconium route.

The presence of a sulfonium salt requires the presence of anionic species. These anions, of which there are at least two, contain a (η^5 : η^1 -C₅H₄CH₂CH₂O)Zr fragment. This is indicated by the triplet signals of the bridging CH₂ hydrogens. Especially for the CH₂O unit a more complex pattern is expected, if there were still a chiral group attached to it. Moreover, the extreme low-field shift of these hydrogens (to ca. 5 ppm) is indicative of a direct Zr–O bond.¹⁹

The species with Cp signals at 6.32 and 6.50 ppm (**A**⁻) seems to be a monoanion (according to NMR integration against signals of the sulfonium moiety). The other species with Cp signals at 6.49 and 6.70 ppm has only half the intensity and must therefore be a dianion (**B**²⁻). We therefore think that **A**⁻ consists of the anion [η^5 : η^1 -C₅H₄CH₂CH₂O)ZrCl₃]⁻. As this species is unsaturated, it seems likely that it will form a six-coordinate μ -OR dimer, as in **6**. Jutzi recently isolated a similar six-coordinate zirconate salt, namely [*trans*-(η^5 -C₅H₄-CH₂CH₂N(H)Me₂)ZrCl₄(pyridine)]₂.^{4c} Accordingly, the ions would combine to form the salt [R₂(isobornyl)S]₂[(η^5 : η^1 - μ -C₅H₄CH₂CH₂O)ZrCl₃]₂ ([S]₂[A]₂). In the reaction of ZrCl₄(THT)₂ with Cp^BSiMe₃ we could indeed isolate such a salt and confirm its constitution by combustion analysis.

The other species **B**²⁻ obviously contains additional inorganic material such as Cl⁻ or more likely ZrCl₅⁻. The latter is corroborated by the fact that thf immediately converts **B** to **A**, probably due to formation and precipitation of ZrCl₅(thf)⁻.²⁰ We therefore think that **B**²⁻ might be the dianion [η^5 : η^1 - μ -C₅H₄CH₂CH₂O)-ZrCl₃(μ -Cl)ZrCl₄]²⁻, ([A](ZrCl₅)]²⁻). This then combines to form a salt of the type [S]₂[(A)(ZrCl₅)]. The anion resembles the known chloride-bridged dianion [Zr₂Cl₁₀]²⁻.²¹ Salts of the type [S]₂[Zr₂Cl₁₀] may have been present in the reaction mixture, but are either insoluble or unstable with respect to comproportionation with the [A]₂ dianion.

The above observations point to the scenario given in Scheme 3. The reaction products are obviously the result of a selective C–O bond scission of the Cp^B ligand. It is evident that coordination of the ether moiety to a ZrCl₄(SR₂) fragment and the extreme stability of the resulting Zr–O bond are responsible for this cleavage.²⁰ One may speculate on the fact whether this cleavage takes place *before* or *after* the formation of the Cp–Zr

(19) (a) Christoffers, J.; Bergman, R. G. *Angew. Chem.* **1995**, *107*, 2423. (b) Rieger, B. *J. Organomet. Chem.* **1991**, *420*, C17. (c) Herrman, W. A.; Morawietz, M. J. A.; Priermeier, T. *Angew. Chem.* **1994**, *106*, 2025.

(20) Atwood, J. L.; Bott, S. G.; Prinz, H. *J. Am. Chem. Soc.* **1986**, *108*, 2113.

(21) Calderazzo, F.; Pallavicini, P.; Pampaloni, G.; Zanazzi, P. F. *J. Chem. Soc., Dalton Trans.* **1990**, 2743.

was slowly added *n*BuLi (10 mL of a 1.6 M solution in hexane). The resulting colorless suspension was cooled to $-30\text{ }^{\circ}\text{C}$, whereupon Me_3SiCl was added (19 mL of a 1.0 M solution in thf). The resulting suspension was stirred for a few hours at room temperature. Water was added (ca. 0.5 mL), and all solvents were removed *in vacuo*. The residue was extracted with pentane and filtered (in air). The combined extracts were evaporated to dryness, affording a yellow viscous oil (4.0 g, 90%). Due to its high boiling point $\text{Cp}^{\text{B}}\text{SiMe}_3$ was used without further purification. $\text{Cp}^{\text{X}}\text{SiMe}_3$ (X = M, F, O) and $\text{Cp}^{\text{B}}\text{SnBu}_3$ were prepared similarly in 80–90% yield. $\text{Cp}^{\text{O}}\text{SiMe}_3$ may be distilled at $80\text{ }^{\circ}\text{C}$ (1 mmHg) but this is not necessary for further applications.

The ^1H and ^{13}C NMR spectra of $\text{Cp}^{\text{X}}\text{SiMe}_3$ (Tables 1 and 2) indicate the presence of only a single isomer, namely 2-alkyl-5-(trimethylsilyl)-1,3-cyclopentadiene.

Synthesis of $\text{Cp}^{\text{O}}\text{TiCl}_3$. To a cooled solution ($-80\text{ }^{\circ}\text{C}$) of $\text{Cp}^{\text{O}}\text{SiMe}_3$ (0.50 g, 2.5 mmol) in 20 mL of CH_2Cl_2 was added TiCl_4 (0.25 mL, 2.2 mmol). The clear solution turned orange immediately. Stirring overnight at room temperature produced orange crystals. After the mixture was cooled to $-80\text{ }^{\circ}\text{C}$, the solids were filtered and washed with 10 mL of pentane; 0.40 g (1.4 mmol, 65%) of product was obtained. Anal. Calcd for $\text{C}_8\text{H}_{11}\text{Cl}_3\text{OTi}$ (277.4): C, 34.6; H, 4.0. Found: C, 33.9; H, 4.7.

Reaction of $\text{Cp}^{\text{X}}\text{SiMe}_3$ (X = B, M, F) with TiCl_4 .
Synthesis of $\text{Cp}^{\text{M}}\text{TiCl}_3$ and $\text{Cp}^{\text{F}}\text{TiCl}_3$. A solution of $\text{Cp}^{\text{M}}\text{SiMe}_3$ (1.59 g, 5.0 mmol) in 15 mL of CH_2Cl_2 was cooled to $-80\text{ }^{\circ}\text{C}$. The addition of TiCl_4 (0.42 mL, 3.8 mmol) resulted in the formation of a clear reddish solution. This solution was gradually warmed to room temperature and evaporated to dryness. The resulting brown oil mainly consists of $\text{Cp}^{\text{M}}\text{TiCl}_3$ (NMR, see Tables 1 and 2). Recrystallization from pentane at $-80\text{ }^{\circ}\text{C}$ affords a yellow solid that melts to a brown oil again below room temperature.

The reaction of $\text{Cp}^{\text{F}}\text{SiMe}_3$ proceeds similarly. The analogous reaction mixture using $\text{Cp}^{\text{B}}\text{SiMe}_3$ gets turbid below room temperature, and no $\text{Cp}^{\text{B}}\text{Ti}$ complexes could be identified after workup.

Synthesis of $[(\eta^5\text{-}\eta^1\text{-C}_5\text{H}_4\text{CH}_2\text{CH}_2\text{OME})\text{ZrCl}_2(\mu\text{-Cl})_2, (\text{Cp}^{\text{O}}\text{ZrCl}_2(\mu\text{-Cl}))_2, \mathbf{2}]$. A solution of $\text{ZrCl}_4(\text{SMe}_2)_2$ in 100 mL of CH_2Cl_2 was prepared *in situ* from ZrCl_4 (6.4 g; 27 mmol) and Me_2S (6 mL, 80 mmol) and filtered to remove a slight amount of insoluble material. This solution was slowly added to a precooled ($0\text{ }^{\circ}\text{C}$) solution of $\text{Cp}^{\text{O}}\text{SiMe}_3$ (5.5 g; 27.5 mmol) in 30 mL of CH_2Cl_2 . The reaction mixture turned red-brown at once. The formation of colorless crystalline material started after 1 h of standing at room temperature. The reaction was left standing overnight. Concentrating and chilling afforded 7.0 g (21.7 mmol, 80%) of product (**2**). Anal. Calcd for $\text{C}_8\text{H}_{11}\text{Cl}_3\text{OZr}$ (320.7): C, 29.9; H, 3.4. Found: C, 29.6; H, 3.7. MS (EI; *m/z*, main peaks of isotope mixture given): 318/320/322 (M^+), 283/285/287 ($[\text{M} - \text{Cl}]^+$), 92 ($\text{C}_5\text{H}_4\text{CH}_2\text{CH}_2^+$).

Reaction of $\text{Cp}^{\text{X}}\text{SiMe}_3$ (X = B, M, F) or $\text{Cp}^{\text{B}}\text{SnBu}_3$ with $\text{ZrCl}_4(\text{SR}_2)_2$. **General Procedure.** A suspension of $\text{ZrCl}_4(\text{SR}_2)_2$ (ca. 2 mmol) prepared *in situ* from freshly sublimed ZrCl_4 and 2–3 equiv of SR_2 in CH_2Cl_2 or toluene (20 mL) was

cooled to $-80\text{ }^{\circ}\text{C}$, and 1 equiv of $\text{Cp}^{\text{X}}\text{SiMe}_3$ (or $\text{Cp}^{\text{B}}\text{SnBu}_3$) was added. As the temperature was raised, an almost clear, dark brown solution was formed that was stirred overnight. After filtration, the solution was evaporated to dryness. The residue was washed with pentane several times, affording a light gray-brown solid. ^1H NMR analysis of this solid in the case of Cp^{M} or Cp^{F} shows a complex pattern of signals in the aliphatic region (1.0–3.5 ppm) which could not be identified. In the case of Cp^{B} defined signals of the isobornyl group were observed, as well as several Cp patterns. After prolonged reaction time or addition of some thf to the initial reaction mixture, only a single compound is left. For $\text{SR}_2 = \text{THT}$, we could isolate a compound of stoichiometry $[\text{THT}(\text{isobornyl})][(\text{C}_5\text{H}_4\text{CH}_2\text{CH}_2\text{O})\text{ZrCl}_3]$ in ca. 95% yield. Anal. Calcd for $\text{C}_{21}\text{H}_{33}\text{Cl}_3\text{OSZr}$ (531.13): C, 47.5; H, 6.3. Found: C, 47.5; H, 6.4.

Synthesis of $[\text{THT}(\text{isobornyl})][\text{O}_3\text{SCF}_3]$. To a cooled ($-80\text{ }^{\circ}\text{C}$) solution of camphene (0.49 g, 3.6 mmol) and THT (0.5 mL, 5.7 mmol) was added HO_3SCF_3 (0.33 mL, 3.7 mmol). The clear colorless solution was gradually warmed to room temperature and evaporated to dryness. The residue was washed twice with pentane and dried *in vacuo*, leaving a white powder. Yield: 1.3 g (95%). Anal. Calcd for $\text{C}_{15}\text{H}_{25}\text{F}_3\text{O}_3\text{S}_2$ (374.49): C, 48.1; H, 6.7; S, 17.1. Found: C, 46.0; H, 6.5; S, 17.5. The ^1H and ^{13}C NMR spectra in CDCl_3 were identical with those of the cation obtained from the reaction of $\text{ZrCl}_4(\text{THT})_2$ and $\text{Cp}^{\text{B}}\text{SiMe}_3$ described above (see Table 6), except that the ^{13}C NMR spectrum shows an additional signal for the O_3SCF_3 anion (120.92 ppm with $^1J_{\text{CF}} = 320\text{ Hz}$).

Ziegler–Natta Polymerization of Ethylene with **2.** A suspension of **2** (2 mg, 6 μmol) and 12 mmol of methylaluminoxane in toluene was filtered and transferred to an autoclave. After 1 h at $70\text{ }^{\circ}\text{C}$ under 4 bar of ethylene, workup yielded 2.7 g of polyethylene. For comparison, $(\eta^5\text{-Cp})_2\text{ZrCl}_2$ yields 160 g of polyethylene under the same conditions.

X-ray Structure Determination of **2.** Data collection was performed with graphite-monochromated Mo $\text{K}\alpha$ radiation ($\lambda = 0.71073\text{ \AA}$) on an Enraf-Nonius MACH III diffractometer, using the $\omega/2\theta$ scan technique. Data were corrected for absorption using ψ -scan data. The structure was solved by direct methods (SHELXS-86). Refinement with anisotropic thermal parameters for non-hydrogen atoms was carried out with full-matrix least-squares techniques (SHELXS-93). H atoms were placed in calculated positions and refined riding.

Acknowledgment. The “Deutsche Forschungsgemeinschaft” is thanked for financial aid. Prof. Dr. K.-H. Thiele is thanked for his continuous support. We thank Dr. Stephan Rosenberger (University of Zürich, Zürich, Switzerland) for performing the low-temperature NMR measurements.

Supporting Information Available: Tables giving details of the data collection, positional and thermal parameters, and bond distances and angles for **2** (6 pages). Ordering information is given on any current masthead page.

OM970040K